Journal of Solid State Chemistry 182 (2009) 3222–3225

Contents lists available at ScienceDirect

Journal of Solid State Chemistry

journal homepage: www.elsevier.com/locate/jssc

Crystal growth and anisotropic magnetic properties of V_3O_7

C. Li, M. Isobe *, H. Ueda, Y. Matsushita, Y. Ueda

Materials Design and Characterization Laboratory (MDCL), Institute for Solid State Physics (ISSP), The University of Tokyo, 5-1-5 Kashiwanoha, Kashiwa, Chiba 277-8581, Japan

ARTICLE INFO

Article history:
Received 18 June 2009
Received in revised form
10 September 2009
Accepted 11 September 2009
Available online 19 September 2009

Keywords:
V_3O_7
Spin-flop
Uniaxial antiferromagnet
Chemical vapor transport
Magnetic anisotropy

ABSTRACT

Needle-like crystals of V_3O_7 up to 2 mm in length were grown by a chemical vapor transport method using NH_4Cl as a transport agent. The anisotropic magnetic susceptibility was measured for the first time. At 2 K, a spin-flop transition occurs under a magnetic field of 0.1 T. V_3O_7 is proved to be a uniaxial antiferromagnet with its easy axis parallel to the *b*-axis of monoclinic structure. A spin structure with antiferromagnetic interaction between $(10\bar{1})$ layers and ferromagnetic interaction in the layers below the Néel temperature (5.2 K) is suggested.

1. Introduction

Vanadium oxides have been attracting considerable attention due to a large variety of vanadium ions' valence states from 2+ to 5+, a rich variety of the structures such as shear structure and various types of polyhedra, and furthermore the interesting properties such as metal-insulator transitions, catalytic ability and so on. However, as for some binary vanadium oxides, studies so far are still not sufficient to understand the physical properties because of the difficulty to synthesize pure sample. Especially, the study of the title compound V_3O_7 has been missing for the past several years.

V_3O_7 is an intermediate phase between VO_2 and V_2O_5 as one of the Wadsley phases with a general chemical formula V_nO_{2n+1} (n=2, 3, 4, … ∞). It is a mixed-valent compound with the ratio of $V^{4+}/V^{5+}=1/2$ and crystallizes into a monoclinic, *C*2/*c*, structure (Fig. 1) [1,2]. V_3O_7 is stable below 950 K as reported previously [3,4].

Physical properties were previously investigated by using polycrystalline samples. V_3O_7 has been reported to be an antiferromagnetic (AF) insulator with the Néel temperature T_N=5.2 K by NMR [5] and neutron scattering study [6]. There is no structural transition down to 4.2 K [7]. According to the measurements of magnetization and NMR, a probable spin structure of V_3O_7 was suggested as a low-dimensional magnetic system with small anisotropy energy; predominant ferromagnetic (F) interaction in the $(10\bar{1})$ layers and long range AF interaction between the layers [5]. However, studies on single crystal are necessary in order to observe the anisotropy and to understand the magnetic ground state. In this paper, we report the details of crystal growth method and the anisotropy of the magnetic properties by using thus obtained V_3O_7 crystal.

2. Experimental

Polycrystalline V_3O_7 was prepared by a solid-state reaction of V_2O_3 and V_2O_5 (4N, RARE METALLIC Co.,). V_2O_3 was prepared by reducing V_2O_5 in H_2 gas at 1173 K for 6 h. The weighed mixture of reagents in the required quantities was pressed into a pellet and heated at 823 K in an evacuated silica tube for 7 days. Thus obtained polycrystalline samples were characterized to be a single phase of V_3O_7 by powder X-ray diffraction (XRD) using Mac Science M21X (Cu*K*α, 40 kV, 300 mA).

Single crystals of V_3O_7 were grown by chemical vapor transport (CVT) method with thus obtained powdered V_3O_7 and various transport agents [8]. The details will appear in the following section. The crystallographic quality of grown crystals was checked by a four-circle diffractometer, RIGAKU AFC-6S X-ray single-crystal diffraction using Mo*K*α X-ray at room temperature.

DC-magnetic susceptibility and field dependence of magnetization were measured by using a Quantum Design MPMS-5T SQUID magnetometer.

3. Results and discussion

3.1. Crystal growth

Different chemicals such as NH_4Cl, I_2, I_2/H_2O and $TeCl_4$ have been examined as the transport agents. The procedures of crystal growth are as follows: Polycrystalline V_3O_7 of 200–300 mg and

* Corresponding author. Fax: +81 0471363436.
E-mail address: isobe@issp.u-tokyo.ac.jp (M. Isobe).

0022-4596/$ - see front matter © 2009 Elsevier Inc. All rights reserved.
doi:10.1016/j.jssc.2009.09.011

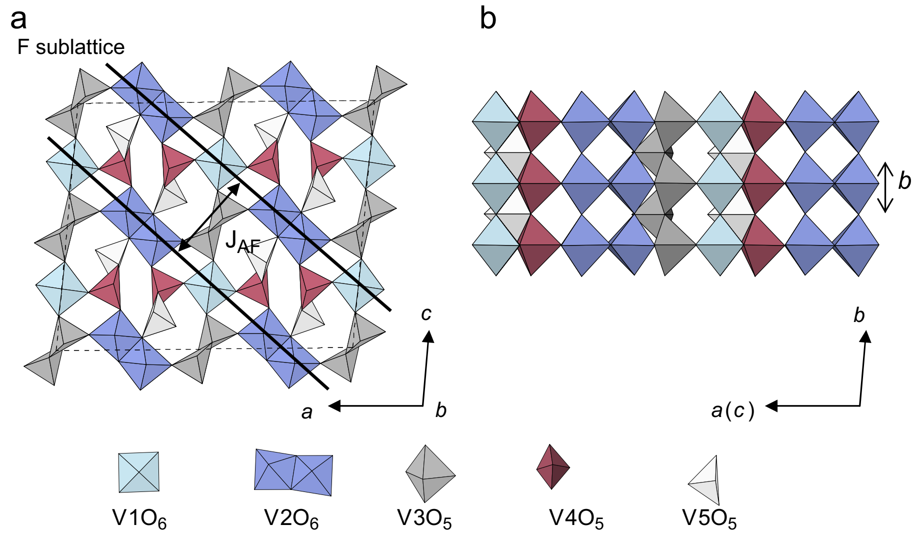

Fig. 1. A view of monoclinic crystal structure of V_3O_7 projected on (0 1 0) (a) and $(10\bar{1})$ (b). The unit cell is composed of 12 octahedra ($V1O_6$ and $V2O_6$), 16 trigonal bipyramids ($V3O_5$ and $V4O_5$) and 8 square pyramids ($V5O_5$). J_{AF} denotes the antiferromagnetic interaction between the $(10\bar{1})$ ferromagnetic layers (F sublattice).

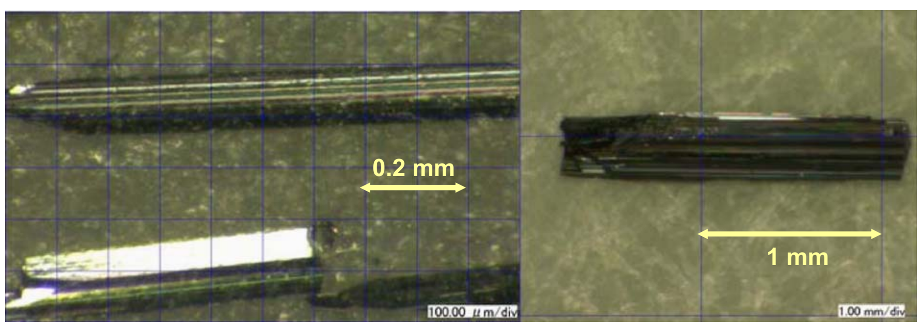

Fig. 2. Crystals of V_3O_7 grown by using NH_4Cl as the transport agent. All the crystals grow along the *b*-axis.

transport agents of 3–5 mg were sealed in an evacuated silica tube with 220 mm in length and 15 mm in diameter, and held for half a month in a four-zone furnace. The temperatures of charge zone and growth zone were adjusted in the range 673–893 K and 623–853 K, respectively. Then the tube was taken out from the furnace and quenched in air. Grown crystals were picked and washed with dilute HCl and deionized water.

In this work, NH_4Cl was proved to be efficient for the growth of V_3O_7 crystal probably due to its relatively high transport efficiency. Attempts to grow crystals via the other three agents were unsuccessful: Any tiny crystals were not formed at the growth zone within half a month probably because of low transport efficiency of I_2 and I_2/H_2O, whereas the accumulation of V_6O_{13} crystals at the growth zone using $TeCl_4$ may be caused by the irreversible formation of TeO_2.

Black needle-like crystals of V_3O_7 were formed under the best growth condition, the temperature gradient of 100 K with the growth zone at 723 K and the charge zone at 823 K. The length of thus obtained single crystals is up to 2 mm, as shown in Fig. 2. All the crystals grow along the *b*-axis parallel to the crystallographic chain. Most of them were found to be twinned with the $(10\bar{1})$ planes by X-ray single-crystal diffraction.

3.2. Magnetic properties

The magnetic susceptibility was measured in the temperature range 2–300 K at the applied magnetic field of 0.1 T parallel ($\chi_{\parallel}$) and perpendicular ($\chi_{\perp}$) to the *b*-axis, respectively (Fig. 3). Both $\chi_{\parallel}$ and $\chi_{\perp}$ show the same behavior of temperature dependence down to 5.2 K and obey a Curie–Weiss law, Eq. (1), above 40 K,

$$\chi(T) = \frac{C}{T-\theta} + \chi_0 \qquad (1)$$

where C is the Curie constant, θ is the Weiss temperature and χ_0 is a temperature-independent term. The best fit provides $C = 0.37$ emu K mol^{-1}, $\theta = 14$ K and $\chi_0 = 8\times10^{-5}$ emu mol^{-1} [9]. The effective moment is thus estimated from C as $\mu_{eff} = 1.72\,\mu_B$ in agreement with the 1.73 μ_B expected for a free V^{4+} ion ($S=\frac{1}{2}$) with the g factor of 1.99 from ESR study [10]. With decreasing temperature lower than 5.2 K, $\chi_{\parallel}$ decreases rapidly, while $\chi_{\perp}$ remains constant as 0.34 emu mol^{-1}. The Néel temperature $T_N = 5.2$ K is the same as that defined in the previous study [6]. The measurements were carried out on the same crystal rotated around the *b*-axis and as a result almost the same $\chi_{\perp}$ was obtained. This means little anisotropic magnetic susceptibility within the *ac*-plane, although the crystal has twin orientation with the $(10\bar{1})$ planes. Hence the anisotropy of the magnetic susceptibility below 5.2 K indicates the typical character of uniaxial antiferromagnet with the easy axis of the *b*-axis.

The magnetic field dependence of magnetization (M) was measured from 0 to 5 T at 2 K. A spin-flop transition occurs at a critical magnetic field of 0.1 T, as clearly seen in Fig. 4. The spin-flop behavior can be understood on the basis of two sublattices. Therefore, the AF exchange interaction, J_{AF}, can be estimated according to Eq. (2) [11] based on molecular

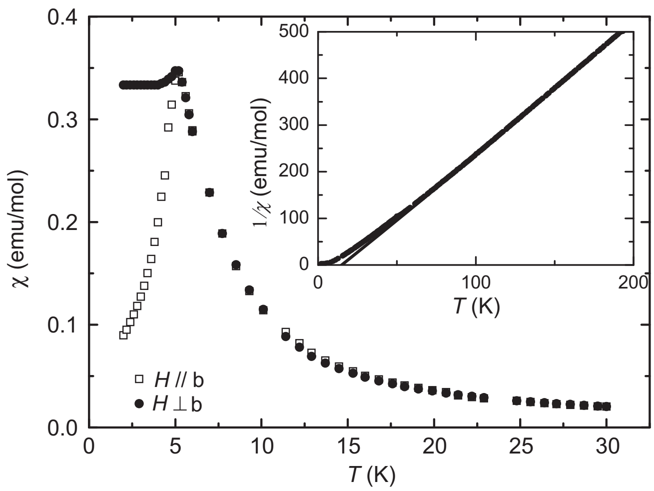

Fig. 3. The temperature dependence of the magnetic susceptibility of V_3O_7 for $H\parallel b$ and $H\perp b$, respectively, at 0.1 T. The inset shows temperature dependence of the reciprocal susceptibility and the fit to the Curie–Weiss law.

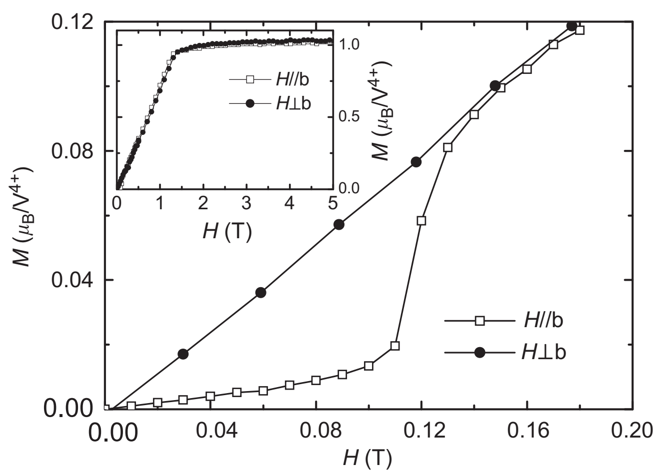

Fig. 4. The magnetic field dependence of magnetization of V_3O_7 at 2 K up to 0.2 T for $H\parallel b$ and $H\perp b$, respectively. The magnetization curve up to 5 T is shown in the inset.

field approximation,

$$A = \frac{1}{\chi_\perp} = \frac{4Z|J_{AF}|}{Ng^2\mu_B^2} \tag{2}$$

where Z is the nearest AF coordination number, A is a constant of molecular field, N is the number of magnetic atoms per mole, g is the Landé g factor calculated as 1.99, and μ_B is the Bohr magneton. $Z|J_{AF}|$ is thus estimated as about 1 K. Furthermore, the critical field of spin-flop transition, H_{SF}, may be written as

$$H_{SF} = [2H_EH_A/(1-\alpha)]^{1/2} \tag{3}$$

where H_E is the exchange field, H_A is the uniaxial anisotropy field (assumed to be small compared to H_E and independent of external field), and $\alpha = \chi_\parallel/\chi_\perp$ [12,13]. The magnitude of the internal field at low temperature may be estimated on the basis of the molecular field theory, which gives

$$\chi_\perp = M_0/(H_E + H_A) \tag{4}$$

where M_0 is the magnetization of the sublattice [12]. By substituting the magnetization data at 2 K, $\chi_\perp$=0.34 emu mol^{-1} and H_{SF}=0.1 T, in Eqs. (3) and (4), one obtains $H_E\sim$0.8 T and $H_A\sim$0.005 T. The spin-flop transition disappears above T_N. As

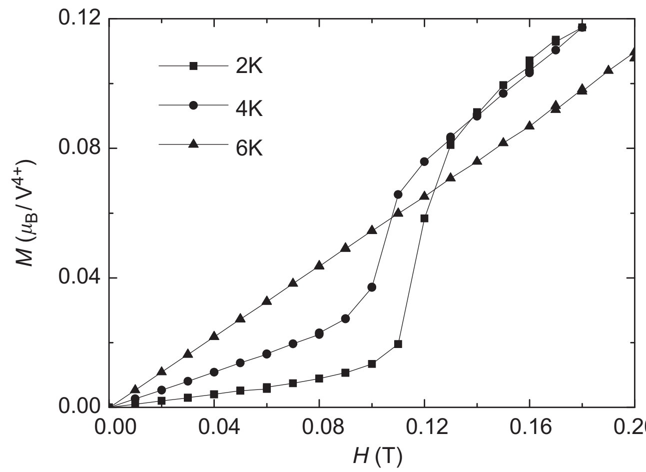

Fig. 5. Isothermal magnetic field-dependent magnetization curves of V_3O_7 at 2, 4 and 6 K for $H\parallel b$.

shown in Fig. 5, the rise of magnetization caused by spin-flop is less marked the closer it is to T_N and is not observed at 6 K.

Above the spin-flop transition, the magnetization gradually increases until it saturates at the critical field, H_C [14]:

$$H_C(T=0) = 2H_E - H_A \tag{5}$$

The estimated critical field hence, $H_C\sim$1.6 T, is close to the observed one, 1.5 T at 2 K determined from the plot of dM/dH (not shown in the present paper). The value of the saturation moment, 1 μ_B per V_3O_7 (the inset in Fig. 4), is consistent with the ionic model of one V^{4+} (S=1/2) ion per V_3O_7.

Next we will discuss the spin structure of V_3O_7 below T_N on the basis of the crystallographic structure and a two-sublattice model by using the information above. There are 12 formula units of V_3O_7 in the unit cell, which is composed of 12 octahedra ($V1O_6$ and $V2O_6$), 16 trigonal bipyramids ($V3O_5$ and $V4O_5$) and 8 square pyramids ($V5O_5$). As shown in Fig. 1(b), corner-sharing VO_6 octahedra form two types of chains, single chains of $V1O_6$ octahedra and double chains of $V2O_6$ octahedra along the b-axis, while edge-sharing VO_5 polyhedra form zigzag strings. Alternate single chains and double chains connected by sharing corners with VO_5 polyhedra form layer structure parallel to $(10\bar{1})$, as shown in Fig. 1(a). The layers are linked by VO_5 zigzag strings then to form a three-dimensional framework [1,15].

The crystallochemical information suggests that the octahedral sites, both the single chain of $V1O_6$ octahedra and the edge-sharing double chains of $V2O_6$ octahedra, are occupied by V^{4+} ions [6].

The V–O bond lengths of each octahedron are about 2.0 Å except one short bond with the length about 1.6 Å. This short length indicates the presence of a vanadyl bond, V=O [16,17], and the local z-axis (d_z-axis in VO_6 octahedra) being parallel to the crystallographic b direction. To avoid the negatively charged oxygen, the off center displacement of the vanadium ion splits the three t_{2g} low energy orbitals into one at lower energy, d_{xy}, and the other two orbitals at higher energy. The d_{xy} orbital hence is occupied by the single d electron of V^{4+} and forms bond with the p_π orbital of the bridging oxygen. Furthermore, the angles of V1–O–V1 and V2–O–V2 along the b-axis are 180° and 175.2°, respectively. According to the Goodenough–Kanamori rule [18], the sign of the d_ε–p_π bond is negative because there is only one d_ε orbital occupied and the exchange integral between the d_ε and p_π orbitals is also negative because the p_π orbital is nonorthogonal to the d_{xy} orbital. Thus the superexchange between V^{4+}–O^{2-}–V^{4+} along the b-axis is considered to be ferromagnetic. This is in good agreement with the conclusion of Ref. [5] and the anisotropic magnetic susceptibility of V_3O_7 crystals, which indicates the existence of an F sublattice. Similar F interaction between V=O…V has been found in many other compounds, such as VO(salpn) [19] and (t-Bupz)$_2$VOCl$_2$ [20]. In general, such kind of classical superexchange interaction via the bridging oxygen always give weak ferromagnetic interaction [21], as reflected in the low positive Curie–Weiss temperature, 14 K.

The maximum of the magnetic susceptibility at T_N is resulted from the magnetic order of the compound. As stated in the earlier part, the magnetization behavior can be understood on the basis of a simplified model of two sublattices with up (+) and down (−) spin, respectively. The molecular field for each sublattice is expressed as [5]:

$$H_E^{\pm} = AM^{\mp} + BM^{\pm},$$

where A is negative (antiferromagnetic) and B is positive (ferromagnetic) constant of molecular field. T_N is given as,

$$T_N = H_E g\mu_B(S+1)/3k_B = (-A+B)(g\mu_B)^2 NS(S+1)/6k_B = 2S(S+1)Z'|J_{T_N}|/3k_B \quad (6)$$

where k_B is the Boltzmann's constant and Z' is the nearest coordination number. $Z'|J_{T_N}|$ is estimated as about 10 K, larger than $Z|J_{AF}|$ (1 K) estimated from $\chi_\perp$. This can be rationalized by the contribution of ferromagnetic interaction between the V^{4+} ions along the b-axis at T_N. The results of the analysis based on two-sublattice model are consistent with those of Ref. [5], in which an AF interaction between $(10\bar{1})$ layers was suggested. Therefore, the spin structure of V_3O_7 can be described as a three-dimensional framework with AF interaction between $(10\bar{1})$ layers and F interaction in the layers.

4. Conclusion

In this study, we successfully grew single crystals of V_3O_7 by CVT method using NH_4Cl as a transport agent, and observed the magnetic anisotropy below T_N for the first time by the magnetization measurements performed on a thus grown crystal. The anisotropic behavior of the temperature dependence of the magnetic susceptibility shows that the easy axis directs parallel to the b-axis. The spin-flop transition at a relatively low field of 0.1 T shows a weak anisotropy in V_3O_7. On the basis of molecular field theory, the exchange field and the uniaxial anisotropy field were calculated as 0.8 and 0.005 T, respectively. A critical field of the saturation of magnetization was thus estimated as about 1.6 T, which is close to the observed one, 1.5 T at 2 K.

In the paramagnetic regime, well above T_N, a Curie–Weiss law was observed with a Curie constant of 0.37 emu K mol^{-1} and a positive Weiss temperature, 14 K. The positive Weiss temperature is rationalized by a ferromagnetic exchange interaction in $(10\bar{1})$ layers within an overall antiferromagnetically ordered system.

Acknowledgments

This study was supported in part by a Grant-in-Aid for Scientific Research (No. 18104008) from the Japan Society for the Promotion of Science (JSPS). C. Li acknowledges JSPS for awarding the Foreigner Postdoctoral Fellowship. The authors also thank T. Yamauchi, K. Ogushi and T. Nakajima for valuable discussion.

References

[1] K. Waltersson, B. Forslund, K. Wilhelmi, Acta Crystallogr. B 30 (1974) 2644.
[2] A. Casalot, Mater. Res. Bull. 7 (1972) 903.
[3] J. Tudo, G. Tridot, C.R. Acad. Sci. Paris 261 (1965) 2911.
[4] T. Toda, K. Kosuge, S. Kachi, Nippon Kagaku Zasshi 87 (1966) 1311 (In Japanese).
[5] H. Nishihara, Y. Ueda, K. Kosuge, H. Yasuoka, S. Kachi, J. Phys. Soc. Jpn. 47 (1979) 790.
[6] A. Heidemann, K. Kosuge, Y. Ueda, S. Kachi, Phys. Stat. Sol. (a) 39 (1977) K37.
[7] M. Bayard, J. Grenier, M. Pouchard, P. Hagenmuller, Mater. Res. Bull. 9 (1974) 1137.
[8] M. Wenzel, R. Gruehn, Z. Anorg. Allg. Chem. 568 (1989) 95.
[9] In order to precisely estimate the parameters of Curie–Weiss law fitting, a large amount of powder sample, compared with the amount of crystals, was used in the magnetic susceptibility measurements.
[10] P.P. Edwards, M.J. Sienko, M. Bayard, Solid State Commun. 21 (1977) 525.
[11] L. Néel, Ann. De Phys. 5 (1936) 232.
[12] T. Nagamiya, K. Yosida, R. Kubo, Adv. Phys. 4 (1955) 1.
[13] L. Holmes, M. Eibschutz, H.J. Guggenheim, Solid State Commun. 7 (1969) 973.
[14] L.J.D. Jongh, A.R. Miedema, Adv. Phys. 50 (2001) 947.
[15] S. Andersson, J. Galy, K. Wilhelmi, Acta Chem. Scand. 24 (1970) 1473.
[16] S.L. Wang, C.Y. Cheng, J. Solid State Chem. 109 (1994) 277; A.C. Dhaussy, F. Abraham, J. Solid State Chem. 126 (1996) 328.
[17] J.W. Pierce, J.B. Goodenough, Phys. Rev. B 5 (1972) 4104.
[18] J.B. Goodenough, Phys. Rev. 115 (1955) 564; J. Kanamori, J. Phys. Chem. Solids 10 (1959) 87.
[19] R.F. Drake, V.H. Crawford, W.E. Hatfield, G.D. Simpson, G.O. Carlise, J. Inorg. Nucl. Chem. 37 (1975) 291.
[20] M. Mohan, M.R. Bond, T. Otieno, C.J. Carrano, Inorg. Chem. 34 (1995) 1233.
[21] M. Tsuchimoto, N. Yoshioka, Chem. Phys. Lett. 297 (1998) 115.